IEEE Access
Multidisciplinary | Rapid Review | Open Access Journal

Received October 27, 2021, accepted November 16, 2021, date of publication November 18, 2021,
date of current version November 30, 2021.

Digital Object Identifier 10.1109/ACCESS.2021.3129191

Potential Function-Based String Stable Controller for Heavy Road Vehicle Platoons

K. B. DEVIKA[1], (Member, IEEE), G. ROHITH[2], (Member, IEEE), AND SHANKAR C. SUBRAMANIAN[1], (Senior Member, IEEE)

[1]Department of Engineering Design, Indian Institute of Technology Madras, Chennai 600036, India
[2]College of Engineering, Mathematics and Physical Sciences, University of Exeter, Exeter EX4 4QF, U.K.

Corresponding author: Shankar C. Subramanian (shankarram@iitm.ac.in)

This work was supported by the Ministry of Skill Development and Entrepreneurship, Government of India, under Grant EDD/14-15/023/MOLE/NILE.

ABSTRACT Heavy Commercial Road Vehicle (HCRV) platooning is a promising solution to meet increasing freight transportation demands. This paper applies the concept of Artificial Potential Functions (APF) to design a string stable controller, viz., Potential Function-based String Stable (PFSS) controller, for establishing stable HCRV platoons under various operating conditions. A methodical approach for the design and selection of potential functions that would maintain the desired intervehicular spacing in the presence of perturbations has been presented. The proposed methodology has been evaluated on a complete vehicle dynamics model-based platoon framework, which would emulate actual vehicle operation. It provides string stable operation under different lead vehicle perturbation maneuvers on various road friction and slope conditions with homogeneous and heterogeneous loading conditions. Compared to existing string stable control approaches, the proposed PFSS controller has attributes such as minimal data requirement from neighboring vehicles, actuator feasible control actions, and simpler control structures.

INDEX TERMS Artificial potential function, heavy commercial road vehicle, platoon, string stability.

I. INTRODUCTION

Heavy Commercial Road Vehicle (HCRV) platoons have the capability in ensuring fuel economic freight movement [1]. In an HCRV platoon, the vehicles travel one after the other with close inter-vehicular distance, such that the aerodynamic drag force between them is minimized, leading to reduced fuel consumption [2], [3]. Moreover, this would lead to efficient utilization of the available road infrastructure [4].

For string stable platoon operation, the spacing error between the vehicles should not propagate along the platoon in the event of a perturbation [5]. An effective string stable controller is crucial for collision-free autonomous platoon operation, and this area has received adequate research attention, as summarized in Table 1.

During string stable controller design, factors such as vehicle dynamics, including aerodynamic drag and rolling resistance, appropriate tire modeling, wheel dynamics, and brake/powertrain actuator dynamics, are significant while considering high-speed vehicle operation. Moreover, these factors are critical in HCRVs due to higher brake actuation delay and response time, higher mass variation during laden and unladen operating conditions, and more significant dynamic load transfer during braking. The current study has considered all these factors. Further, the variation in road friction coefficient (μ) has been considered to incorporate operation in different road conditions. Vehicles of different masses are also considered to characterize the heterogeneity in loading conditions that can be seen in HCRV platoons. The effect of road gradients on string stability has also been investigated since these are encountered in long haul operations. From Table 1, existing studies on string stable controllers have not explicitly considered all the aforementioned factors. In this context, the current study attempts to incorporate all these factors in the string stable control design for HCRV platoons using an Artificial Potential Function (APF) approach.

APF has been widely used in modelling interaction among robots and their environment [29]–[35]. Recent research applied APF for automotive applications [10], [11], [26], [36]. In [10], the APF control approach has been used for designing an automated driving strategy by integrating cooperative adaptive cruise control with collision avoidance and gap closing functionalities. APF has been used to design

The associate editor coordinating the review of this manuscript and approving it for publication was Nasim Ullah.

TABLE 1. A brief summary of research in road vehicle platooning in the last ten years.

S.No.	Study	Vehicle dynamics	μ / W / θ variations	Controller
1.	Tuchner et al. [6]	✗	✗ / ✗ / ✗	Interpolating
2.	Ploeg et al. [7]	✗	✗ / ✗ / ✗	H_∞
3.	Guo et al. [8]	✗	✗ / ✗ / ✗	SMC
4.	Merco et al. [9]	✗	✗ / ✗ / ✗	Hybrid
5.	Kazerooni et al. [10]	✗	✗ / ✗ / ✗	APF
6.	Kazerooni et al. [11]	✗	✗ / ✗ / ✗	APF
7.	Kianfar et al. [12]	✗	✗ / ✗ / ✗	MPC
8.	Naus et al. [13]	✗	✗ / ✗ / ✗	Feedforward
9.	van Nunen et al. [14]	✗	✗ / ✗ / ✗	MPC + Feedforward
10.	Peng et al. [15]	✗	✗ / ✗ / ✗	SMC
11.	Xiao et al. [16]	✗	✗ / ✓ / ✗	SMC
12.	Dunbar et al. [17]	✗	✗ / ✓ / ✗	Receding horizon
13.	Németh et al. [18]	✗	✗ / ✗ / ✓	H_∞
14.	Chen et al. [19]	✗	✗ / ✗ / ✓	FSF
15.	Kwon et al. [20]	✓	✗ / ✗ / ✗	SMC
16.	Dolk et al. [21]	✓	✗ / ✗ / ✗	Event triggered
17.	Liang et al. [2]	✓	✗ / ✗ / ✓	Optimal
18.	Zhai et al. [22]	✓	✗ / ✗ / ✓	MPC
19.	Guo et al. [23]	✓	✗ / ✗ / ✓	Adaptive SMC
20.	Xu et al. [24]	✓	✗ / ✗ / ✓	H_∞
21.	Gao et al. [25]	✓	✗ / ✓ / ✗	H_∞
22.	Yang et al. [26]	✓	✗ / ✓ / ✓	APF
23.	Zhai et al. [27]	✓	✗ / ✓ / ✓	MPC
24.	Devika et al. [28]	✓	✓ / ✓ / ✗	SMC
25.	**Current study**	✓	✓ / ✓ / ✓	APF

μ - Road friction coefficient, W - Vehicle weight, θ - Road gradient.

a longitudinal control scheme for the cooperative merging of car platoons [11]. Feng *et al.* used APF for generating safe collision-free paths for autonomous vehicles [36]. A hierarchical control scheme for fuel-efficient and collision-free car platoons using dynamic programming and APF has been presented in [26].

In [28], the authors have incorporated factors such as vehicle dynamics and μ variations in the design of string stable controllers for HCRV platoons using sliding mode control. However, like other commonly used approaches, the controller demands individual vehicle's position, speed, and/or acceleration information from both the preceding and succeeding vehicles [8]. The practical implementation of such control methods would be highly sensing dependent. Motivated by these factors, this paper designs a string stable controller with lower data requirements from neighboring vehicles by utilizing the concept of APF. The Potential Function-based String Stable (PFSS) controller has been proposed such that it would require position and speed information from the preceding vehicle alone.

The proposed PFSS controller would synthesize control inputs (acceleration/deceleration commands) for each individual vehicle in the platoon based on instantaneous spacing and speed errors, such that the spacing error is attenuated along the platoon. The idea is to decelerate the vehicle when the inter-vehicular distance between the constituent HCRVs in the platoon becomes less than the desired threshold value to avoid collisions and accelerate the vehicle when the inter-vehicular distance becomes more than the desired threshold. Since the proposed approach does not incorporate the error propagation factor directly into the controller design as in conventional controllers [8], [28], the controller structure becomes simpler, making practical implementation easier.

The major attributes of the proposed PFSS controller, viz., error attenuation capability, minimal data requirement from the neighboring vehicles, and ability to synthesize actuator feasible control inputs, have been investigated by comparing its performance with the commonly used sliding mode based string stable controller. Further, the proposed PFSS controller has been tested extensively for its efficacy under different operating scenarios.

II. VEHICLE MODEL

The platoon is assumed to have $N+1$ vehicles, with one leader and N followers (Fig. 1). The following assumptions were made in this study:

- Only longitudinal dynamics of the HCRV has been considered.
- The tire model parameters and vehicle parameters were assumed to be known.
- Equal load distribution on the left and the right wheel of a specific axle of the vehicle was assumed.

A. HCRV MODEL

The equation that characterizes the leader vehicle motion is

$$\dot{x}_0(t) = v_0(t), \tag{1}$$

where, $x_0(t)$ and $v_0(t)$ are the position and longitudinal speed of the leader vehicle, $v_0(t)$ being the speed that has to be followed by the follower vehicles.

The position and longitudinal speed dynamics of the i^{th} follower vehicle are represented as

$$\begin{aligned} \dot{x}_i(t) &= v_i(t), \\ \dot{v}_i(t) &= \Omega(v_i(t), \tau_{ji}(t)), \end{aligned} \tag{2}$$

where, $\tau_{ji}(t)$ is the drive/brake input with $j = f, r$, indicating front and rear wheels, respectively, and $\Omega(v_i(t), \tau_{ji}(t))$ represents a nonlinear function in $v_i(t)$ and $\tau_{ji}(t)$, which is given by

$$\Omega(v_i(t), \tau_{ji}(t)) = \frac{1}{m_i}\left(\sum_{j=f,r} F_{xji}(\lambda_{ji}(t), \tau_{ji}(t)) - F_{Ri}(t)\right). \tag{3}$$

The mass of the i^{th} follower vehicle is represented by m_i. $F_{xji}(\lambda_{ji}(t), \tau_{ji}(t))$ represents the longitudinal force at the tire-road interface and is a function of the longitudinal wheel slip ratio, $\lambda_{ji}(t)$, the friction coefficient (μ) between the tire and the road, and the normal load on the tire ($F_{zji}(t)$) [37]. These are characterized by

$$\lambda_{ji}(t) = \begin{cases} \dfrac{v_i(t) - r_{ji}\,\omega_{ji}(t)}{v_i(t)}, & \text{during braking,} \\ \dfrac{r_{ji}\,\omega_{ji}(t) - v_i(t)}{r_{ji}\,\omega_{ji}(t)}, & \text{during drive,} \end{cases}$$

$$\dot{\omega}_{ji}(t) = \frac{1}{I_{ji}}(\tau_{ji}(t) - r_{ji}F_{xji}(t)),$$

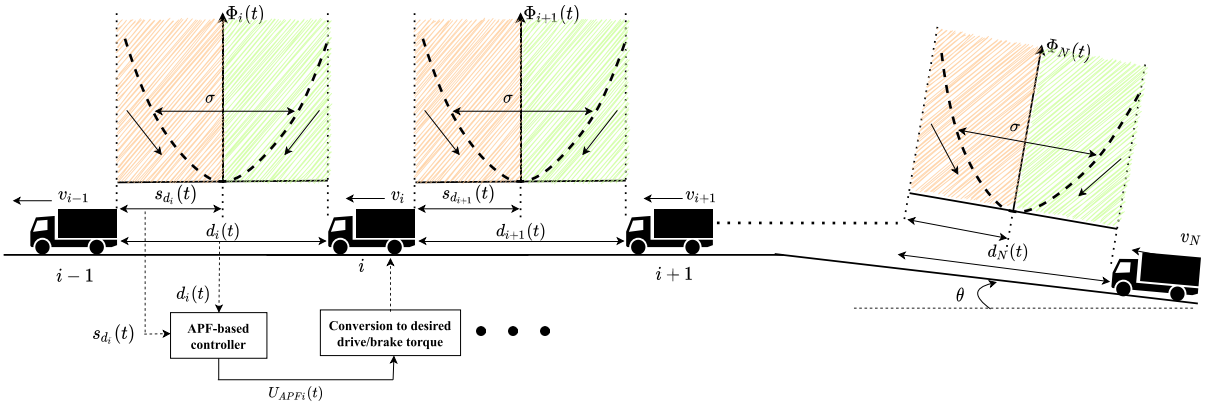

FIGURE 1. HCRV Platoon operation via APF action.

$$F_{zfi}(t) = \frac{m_i(g(l_{ri}\cos\theta - h_i\sin\theta) - a_i(t)h_i) - F_{ai}(t)\,h_{ai}}{l_{fi}+l_{ri}},$$
$$F_{zri}(t) = \frac{m_i(g(l_{fi}\cos\theta + h_i\sin\theta) + a_i(t)h_i) + F_{ai}(t)\,h_{ai}}{l_{fi}+l_{ri}}, \quad (4)$$

where, r_i is the tire radius, and ω_{ji} represents the angular speed of the wheels, I_{ji} represents the moment of inertia of wheels, $a_i(t)$ represents the longitudinal acceleration, h_i is the height of the Center of Gravity (CG) of the vehicle, and h_{ai} is the height of the location at which the equivalent aerodynamic force acts. The longitudinal distances of the front and rear axles from the CG of the vehicle are represented by l_{fi} and l_{ri}, respectively. The road gradient is represented by θ and is defined to be positive for an up-grade and negative for a down-grade.

Using the Magic Formula (MF) tire model [38], the longitudinal force at the tire-road interface is represented as,

$$F_{xji}(\lambda_{ji}(t)) = D\sin(C\tan^{-1}(\Gamma - E(\Gamma - \tan^{-1}\Gamma))) + S_V, \quad (5)$$

where, $\Gamma = B\lambda_x(t)$, and $\lambda_x(t) = \lambda_{ji}(t) + S_H$.

In this study, the MF model parameters, B, C, D, E, S_H, S_V were obtained from the vehicle dynamic simulation software, IPG TruckMaker®.

The resistive force on the i^{th} vehicle, $F_{Ri}(t)$, is given by

$$F_{Ri}(t) = -m_i g(f_i\cos\theta + \sin\theta) - \rho a_{fi} C_{Di}(t)\frac{v_i(t)^2}{2}, \quad (6)$$

where, f_i is the rolling friction coefficient, ρ is the air density, a_{fi} is the vehicle frontal area, and C_{Di} is the drag coefficient.

The transfer function of the air brake system developed by Sridhar *etal*. [39] via Hardware in Loop experimentation is

$$P_{ji}(s) = \frac{\tau_{ji}(s)}{\tau_{desji}(s)} = \frac{1}{1+\delta_{dji}s}e^{-T_{dji}s}, \quad (7)$$

where, δ_{dji} is the time constant, and T_{dji} is the time delay, and τ_{desji} and τ_{ji} represent the demanded brake torque and actual brake torque developed, respectively. The experimentally corroborated values for the model parameters as given in [39] are $\delta_{dji} = 260$ ms and $T_{dji} = 45$ ms, and these have been utilized in this study. Literature suggests using a first-order model with a time constant and delay for approximating the powertrain dynamics during the acceleration/drive phase [40]. Hence, a similar model as presented in Eq. (7) has been used to incorporate actuation dynamics in the drive phase. Literature supports the use of $\delta_{dji} = 260$ ms and $T_{dji} = 45$ ms as feasible choices during acceleration/drive phase as well [40].

The first order Padé approximation has been used to represent Eq. (7) as

$$P_{ji}(s) \approx \frac{(2 - T_{dji}s)}{(1+s\delta_{dji})(2+T_{dji}s)}. \quad (8)$$

The state space representation of Eq. (8) can be written as

$$\begin{bmatrix}\dot{\eta}_{1ji}(t)\\ \dot{\eta}_{2ji}(t)\end{bmatrix} = \begin{bmatrix}0 & 1\\ \frac{-2}{\tau_d T_d} & -(\frac{1}{\tau_d}+\frac{2}{T_d})\end{bmatrix}\begin{bmatrix}\eta_{1ji}(t)\\ \eta_{2ji}(t)\end{bmatrix} + \begin{bmatrix}0\\1\end{bmatrix}\tau_{desji}(t), \quad (9)$$

$$\tau_{ji}(t) = \begin{bmatrix}\frac{2}{T_d\tau_d}\\ \frac{-1}{\tau_d}\end{bmatrix}\cdot\begin{bmatrix}\eta_{1ji}(t)\\ \eta_{2ji}(t)\end{bmatrix}. \quad (10)$$

Now, on substituting $\eta_{1ji}(t)$, $\eta_{2ji}(t)$ from (10) in (4), the rotational dynamics of the wheels can be expressed as

$$\dot{\omega}_{ji}(t) = \frac{1}{I_{ji}}\Big(\frac{2}{T_d\tau_d}\tau_{1ji}(t) - \frac{1}{\tau_d}\tau_{2ji}(t) - r_i F_{xji}(t)\Big), \quad (11)$$

Considering this complete vehicle model including actuator dynamics, each follower vehicle's dynamics in the platoon can be represented as

$$\dot{\boldsymbol{\Upsilon}}_i(t) = \mathbf{f}(\boldsymbol{\Upsilon}_i(t), \mathbf{u}_i(t)), \quad (12)$$

where, $\boldsymbol{\Upsilon}_i(t) = \big[x_i(t)\ v_i(t)\ \omega_{fi}(t)\ \omega_{ri}(t)\ \eta_{1fi}(t)\eta_{2fi}(t)\ \eta_{1ri}(t)\ \eta_{2ri}(t)\big]^T$ is the state vector, and $\mathbf{u}_i(t) = \big[\tau_{desfi}(t)\ \tau_{desri}(t)\big]^T$ is the input vector.

III. ARTIFICIAL POTENTIAL FUNCTION BASED STRING STABLE CONTROLLER

A. CONCEPT OF ARTIFICIAL POTENTIAL FUNCTION

Artificial Potential Functions (APFs) are used to represent the virtual energy level of physical systems and have been

widely used for path planning in robotic systems [29]–[32]. In this approach, all entities in the configuration space are assumed to be carrying potential charges, both attractive and repulsive. By properly selecting these potentials, it would be possible to regulate vehicle movements and have a collision-free operation. In order to achieve this, a positive definite "artificial potential", $\Phi(\mathbf{S}) : \Re^n \rightarrow \Re$, is defined, where $\mathbf{S} \in \Re^n$ is the state of the dynamical system. The potential function, $\Phi(\mathbf{S})$ could consist of both attractive ($\Phi_a(\mathbf{S})$) and repulsive ($\Phi_r(\mathbf{S})$) components, that regulate the vehicle behavior.

A significant advantage of APF-based approaches is that they could provide a simple but flexible mechanism to integrate multiple design requirements and constraints while ensuring closed-form solutions [10], [11]. For instance, it is desirable to keep the vehicles at a minimum intervehicular distance in platoon applications. In case of any perturbation, this would require continuous adjustment of the vehicle position. A potential function, $\Phi(\mathbf{S})$ is an energy-like function and can be designed to have a minimum value at the desired intervehicular distance. If vehicles become close to each other (spacing less than desired value), the repulsive field should push them towards the desired intervehicular distance, avoiding collisions. Conversely, if they become far apart, the attractive potential should move them towards the desired distance. This can be achieved by using control inputs derived using the gradient of the potential function. Hence, using APF, the desired (equilibrium) intervehicular distances could be maintained, ensuring a stable platoon operation.

B. ERROR DYNAMICS

From Fig. 1, the spacing between a pair of vehicles in the platoon at each time instant is given by,

$$d_i(t) = x_{i-1}(t) - x_i(t). \tag{13}$$

Every follower vehicle in the platoon should follow the preceding vehicle with a desired inter-vehicular spacing given by

$$s_{d_i}(t) = s_o + h_i v_i(t), \tag{14}$$

where, s_o and h_i represent standstill spacing and the time-headway respectively. To avoid collision between two consecutive vehicles, a follower vehicle should follow its preceding vehicle's speed profile (since $s_{d_i(t)}$ is a function of $v_i(t)$). Hence the control objective in a string stable controller design problem is

$$\begin{aligned} d_i(t) &\rightarrow s_o + h_i v_i(t), \\ v_i(t) &\rightarrow v_{i-1}(t). \end{aligned} \tag{15}$$

Given a perturbation, the spacing error between two consecutive vehicles is,

$$e_i(t) = d_i(t) - s_{d_i}(t). \tag{16}$$

For string stability, $e_i(t) \rightarrow 0$ by making $d_i(t) \rightarrow s_{d_i}(t)$, and this could be achieved through,

$$\begin{aligned} &\text{if } e_i(t) > 0, \ \& \ d_i(t) > s_{d_i}(t), \ \text{then } \dot{v}_i(t) > 0, \\ &\text{if } e_i(t) < 0, \ \& \ d_i(t) < s_{d_i}(t), \ \text{then } \dot{v}_i(t) < 0. \end{aligned} \tag{17}$$

An augmented error function ($\Psi_i(t)$) is defined as,

$$\Psi_i(t) = \kappa e_i(t) + \dot{e}_i(t), \tag{18}$$

where, κ is a positive real number, and $\Psi_i(t)$ considers error in both intervehicular distance and longitudinal speed. The value of $\Psi_i(t)$ would be zero for a platoon in equilibrium.

C. PROPERTIES OF THE POTENTIAL FUNCTION

For a continuous and differentiable function $\Phi_i(t) = f(\Psi_i(t))$, where, $\Psi_i(t)$ is a function of the intervehicular spacing $d_i(t)$,

1) THE FUNCTION SHOULD HAVE GLOBAL MINIMA AT THE DESIRED INTERVEHICULAR DISTANCE, $s_{d_i}(t)$

To maintain the follower vehicles at a desired intervehicular distance, $\Phi_i(t)$ should satisfy

$$\begin{aligned} &\frac{d\Phi_i(t)}{d\Psi_i(t)}|_{\Psi_i(t)=0} = 0, \\ &\frac{d^2\Phi_i(t)}{d\Psi_i^2(t)}|_{\Psi_i(t)=0} > 1. \end{aligned} \tag{19}$$

The goal is to maintain the intervehicular spacing $d_i(t)$ at $s_{d_i}(t)$ ($\Psi_i(t) = 0$). Since the control input is computed as the gradient of the potential function, the follower vehicle would move towards the minimum energy point. If the vehicle is perturbed from this point, the vehicle would be automatically brought back by acceleration/braking.

2) THE FUNCTION SHOULD BE (STRICTLY) MONOTONOUSLY DECREASING IN THE RANGE $(0, s_{d_i}(t)]$

In a scenario where the follower vehicle moves closer to the preceding vehicle, such that the intervehicular spacing is below the threshold value (and could cause collisions), brakes should be applied. The speed reduction (and brake force) should be higher as the follower vehicle is closer to the vehicle in front and should decrease as it moves away towards the desired intervehicular distance. This could be ensured by choosing the potential function to satisfy

$$\begin{aligned} &\frac{d\Phi_i(t)}{d\Psi_i(t)} < 0, \quad (0, s_{d_i}(t)], \\ &\lim_{d_i(t)\rightarrow 0} \Phi_i(t) > \lim_{d_i(t)\rightarrow s_{d_i}(t)} \Phi_i(t). \end{aligned} \tag{20}$$

When the function is monotonically decreasing as presented by equation (20), the control input (as gradient of potential function $\frac{d\Phi_i(t)}{d\Psi_i(t)}$) would have negative values, indicating braking, and thus avoiding collisions.

3) THE FUNCTION SHOULD BE (STRICTLY) MONOTONOUSLY INCREASING IN THE RANGE $[s_{d_i}(t), \infty)$

A converse scenario exists in which the follower vehicle is further away from the preceding vehicle, with a spacing value much higher than the desired intervehicular distance. In such a condition, the follower vehicle should accelerate and move towards the preceding vehicle. The spacing error should be

reduced quickly, and this is achieved by ensuring

$$\frac{d\Phi_i(t)}{d\Psi_i(t)} > 0, \quad [s_{d_i}(t), \infty)$$
$$\lim_{d_i(t)\to s_{d_i}(t)} \Phi_i(t) < \lim_{d_i(t)\to\infty} \Phi_i(t). \tag{21}$$

When the function is monotonically increasing as presented by equation (21), the control input has positive values, indicating acceleration, thus maintaining the platoon formation.

To achieve these properties, a parabolic potential function is chosen as a candidate function in this study.

Proposition 1: For the error function presented in Eq. (18) and for the system under study, the choice of $\Phi_i(t) = \frac{1}{2}\sigma_i\Psi_i(t)^2$ *would satisfy the above properties for* $\sigma_i > 0$.

Proof: The selected potential function should satisfy the aforementioned three properties.

EXISTENCE OF GLOBAL MINIMA

It can be noted that,

$$\frac{d\Phi_i(t)}{d\Psi_i(t)}|_{d_i(t)=s_{d_i}(t)} = 0. \tag{22}$$

Checking the second derivative,

$$\frac{d^2\Phi_i(t)}{d\Psi_i^2(t)}|_{d_i(t)=s_{d_i}(t)} = \sigma_i > 0, \quad \forall\, \sigma_i, \tag{23}$$

Thus, the function is minimum at $d_i(t) = s_{d_i}(t)$.

MONOTONICITY

To check the monotonicity, one should check for the sign of $\frac{d\Phi_i(t)}{d\Psi_i}$ in the intervals as mentioned in Eqs. (20) and (21). In the interval $(0, s_{d_i}(t)]$, $e_i(t) < 0$, and $\dot{e}_i(t) < 0$, making $\frac{d\Phi_i(t)}{d\Psi_i} < 0$. In this interval, the i^{th} vehicle is closer to the $(i-1^{th})$ vehicle and has to decelerate to maintain the desired $d_i(t)$. Similarly, in the interval $[s_{d_i}(t), \infty)$, $e_i(t) > 0$, and $\dot{e}_i(t) > 0$, making $\frac{d\Phi_i(t)}{d\Psi_i} > 0$, and the vehicle has to accelerate to make $d_i(t) = s_{d_i}(t)$.

□

D. PFSS CONTROLLER DESIGN FOR STRING STABLE OPERATION

The gradient of $\Phi_i(t)$ is taken with respect to $\Psi_i(t)$ and used to obtain the acceleration/deceleration control input as,

$$u_{APF_i}(t) = \frac{\partial\Phi_i(t)}{\partial\Psi_i(t)} = \sigma_i\Psi_i(t). \tag{24}$$

Now, substituting Eqs. (14), (13), (16), and (18), in Eq. (24),

$$u_{APF_i}(t) = \sigma_i\Big(\kappa(x_{i-1}(t) - x_i(t) - s_o - h_i v_i(t)) + v_{i-1}(t) - v_i(t) - h_i\dot{v}_i(t)\Big). \tag{25}$$

Algorithm 1 presents the PFSS control methodology. It is to be noted that, for the realization of the control equation described by Eq. (25), only the position and speed information from the preceding $(i-1)^{th}$ vehicle is required in addition to that of the i^{th} vehicle. The control equation does not require information from the succeeding $(i+1)^{th}$ vehicle. Moreover, this approach does not require acceleration information from the $(i-1)^{th}$ vehicle. Now, the total desired torque can be obtained as,

$$\tau_{desi}(t) = \begin{cases} m_i r_i u_{APF_i}(t), & \text{for } \tau_{desi}(t) < \tau_{sati}, \\ \tau_{sati}, & \text{for } \tau_{desi}(t) \geq \tau_{sati}, \end{cases} \tag{26}$$

where, τ_{sati} represents the saturation magnitude characterizing the maximum physical limits of the actuator. During acceleration (since HCRVs are typically rear wheel driven),

$$\tau_{desfi}(t) = 0,$$
$$\tau_{desri}(t) = \tau_{desi}(t). \tag{27}$$

During braking,

$$\tau_{desfi}(t) = \beta\tau_{desi}(t),$$
$$\tau_{desri}(t) = (1-\beta)\tau_{desi}(t), \tag{28}$$

where, β represents the torque distribution factor between front and rear wheels.

Algorithm 1 PFSS Control Algorithm

Step 1: Initialize $x_i(0)$, $v_i(0)$, $d_i(0)$, h_i, s_o, $s_{d_i}(0)$;
Step 2: Get road and loading parameters, μ, θ, and W;
Step 3: Use dynamic vehicle model presented using equation (12) to update $x_i(t)$ and $v_i(t)$ values;
Step 4: Compute error $e_i(t)$ using equation (16);
Step 5: Compute augmented error function $\Psi_i(t)$ using equation (18);
Step 6: **Function** `PFSS` $(\Psi_i(t))$ **:**
  Step 7: Define $\Phi_i(t) = f(\Psi_i(t))$, satisfying properties presented in Section III-C;
  Step 8: Compute $u_{APF_i}(t)$ using equations (24) and (25);
  Step 9: Compute torque inputs using equations (26) and (27) or (28);
  Step 10: return $\tau_{desfi}(t)$, $\tau_{desri}(t)$;
Step 11: Go to **Step 2**;

IV. RESULTS AND DISCUSSIONS

A. TEST CONDITIONS

A platoon of 5 HCRVs (one leader plus four follower configuration) has been considered. The vehicle parameters used in [28] were adopted here. The platoon leader was assumed to undergo an accelerating maneuver from 10 m/s to 15 m/s and a decelerating maneuver from 10 m/s to 5 m/s. Two different rates of 1 m/s^2 and 2 m/s^2 were considered. Both dry and wet road conditions, corresponding to μ values of 0.8 and 0.4, respectively, were used in the study. Road slopes (θ) of $-5°$, $0°$, and $+5°$, indicating downhill, straight and uphill operating conditions, respectively, in accordance with [41], were considered. The test cases were simulated using $\sigma_i = \sigma$ for all the follower vehicles. To test the efficacy of the controller, a limiting scenario where the platoon leader

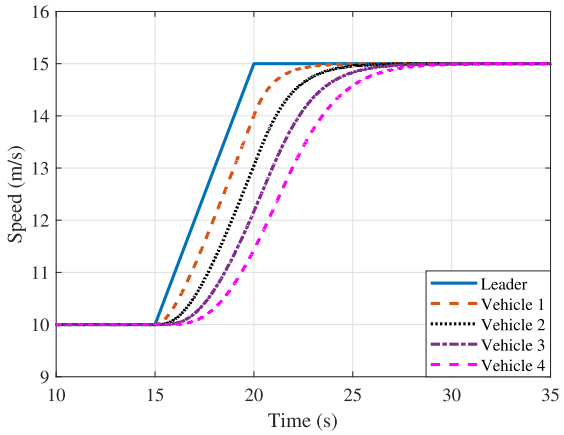

FIGURE 2. Follower vehicles speed tracking profiles for an accelerating leader on an uphill road.

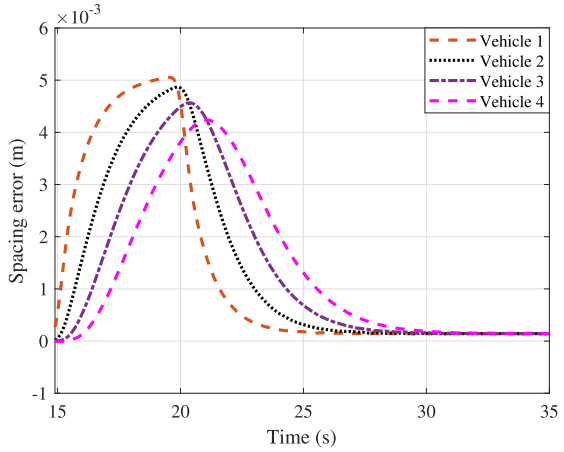

FIGURE 3. Plots showing spacing error attenuation.

undergoes an acceleration maneuver on an uphill road is considered, and plots and analyses corresponding to the same are presented next. Results corresponding to other sets of operating conditions have been presented in Table 2.

B. PERFORMANCE EVALUATION OF PFSS CONTROLLER

Figure 2 presents the scenario where the platoon leader undergoes an acceleration maneuver on an uphill road. The maneuver starts at $t = 15$ s and ends at $t = 20$ s, with leader having an acceleration of 1 m/s^2. The follower vehicles were found to be following the leader, ensuring a stable platoon operation. Figure 3 presents the spacing error attenuation plots for the speed tracking profiles presented in Fig. 2. The spacing errors were found to be attenuating along the platoon length (96%, 90%, and 84% of the first vehicle error magnitude). The magnitude of the instantaneous spacing errors was found to be in the order of millimeters, which is negligible compared to the size of the vehicle.

C. COMPARISON WITH CONVENTIONAL STRING STABLE CONTROLLERS

To establish the efficacy of the proposed PFSS controller over existing string stable controllers, it has been compared

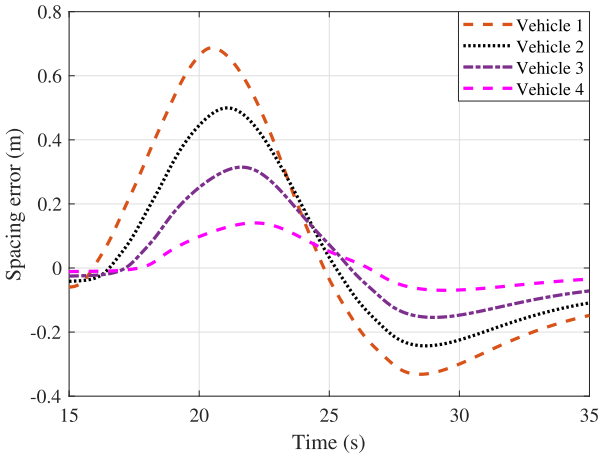

FIGURE 4. Spacing error attenuation plots using conventional model based approach.

with the well-established sliding mode-based string stable control design approach [8], [28]. Due to the simple control structure as presented in Eq. (25), the proposed PFSS controller requires tuning of only two parameters (σ_i, κ), whereas conventional design approaches presented in [8] and [28] require a minimum of five and seven parameters to be simultaneously tuned to ensure string stable operation. Further, different aspects, viz., error attenuation capability, performance under actuator constraints, and lower data requirement, have been analyzed and compared to show the advantages of the proposed PFSS controller.

1) ERROR ATTENUATION CAPABILITY

The same scenario as presented in Section 2 has been considered using the sliding mode approach [28] for comparison, and the corresponding error attenuation profile is presented in Fig. 4. Even though string stable operation was achieved, the magnitude of spacing error values was found to be much higher (approximately three orders of magnitude higher) compared to the proposed approach (Fig. 3). In addition to this, using the sliding mode approach, the magnitude of the torque required was also found to be much higher compared to that of the proposed APF methodology (Fig. 5). The control input exceeded the actuator limit with the SMC controller. The error plots presented in Fig. 4 have been generated by relaxing the actuator constraints. The sliding mode-based approach used an augmented error propagation function as the switching function, and the controller has been designed to attenuate the error propagation. On the other hand, the proposed APF approach does not consider error propagation terms in the control design and maintains the string stability by mitigating individual intervehicular errors instantaneously. This prevents the errors from growing to higher values. As soon as a non-zero error exists, the controller would try to mitigate it by either accelerating/decelerating the vehicles.

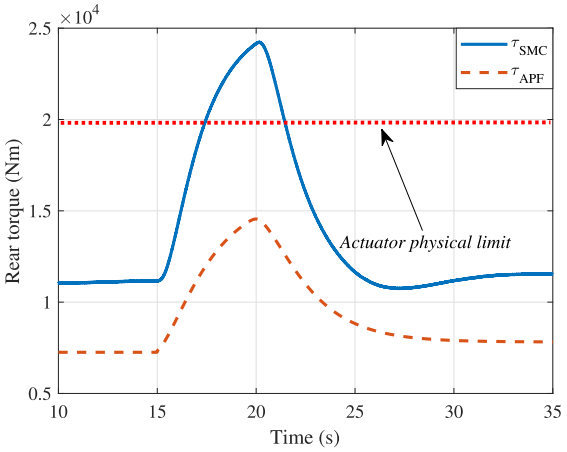

FIGURE 5. Vehicle 1 rear torque input for tracking the profile shown in Fig. 2.

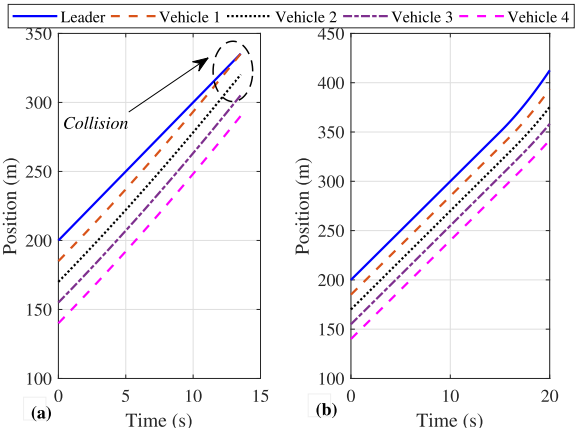

FIGURE 6. Position plots with communication latency; (a). conventional controller, (b). PFSS controller.

2) PERFORMANCE UNDER ACTUATOR CONSTRAINTS

Figure 5 presents rear torque input profiles of the (follower) vehicle 1 (for both PFSS and conventional SMC controllers) for tracking the speed profile as presented in Fig. 2. The maximum permissible torque value (obtained from the vehicle datasheet and IPG TruckMaker® software), limited by the actuator physical constraints, is also marked. The plot shows that the torque inputs are well within the actuator's limits with the proposed controller and are practically realizable. On the other hand, if one were to use a conventional approach as presented in [28], the computed torque inputs were found to exceed the aforesaid actuator physical limit. When the actuator constraints were strictly imposed, then the corresponding torque inputs were not sufficient to track a lead vehicle perturbation (as presented in Fig. 2) and resulted in collisions.

3) DATA REQUIREMENT AND STABILITY

The control equation (Eq. (25)) for the PFSS controller is a function of the position and speed information of the $(i-1)^{th}$ and the i^{th} vehicles alone, $u_i(t) = f(x_{i-1}(t), x_i(t), x_{i-1}(t), x_i(t))$. However, well-established string stable control design approaches would require data from preceding and succeeding vehicles [8], [28]. In order to demonstrate the impact of reduced data requirement from neighboring vehicles, the same scenario as presented in Fig. 2 has been evaluated using the PFSS controller in the presence of a communication delay. It was assumed that a constant communication delay of 100 ms was present during data transmission from the neighboring vehicles [42]. A conventional controller as presented in [28] has also been used to track the same profile. From the results, one can observe that using the conventional control strategy, communication delay during data transmission from preceding and succeeding vehicles resulted in string instability as presented in Fig. 6 (a). However, the proposed PFSS controller could maintain string stability even with the delay in data transmission from the preceding vehicles (Fig. 6 (b)). It is interesting to note that the conventional controller could maintain a stable operation if the same communication delay were assumed to be present only during data transmission from the preceding vehicle [28], signifying the importance of minimal data requirement.

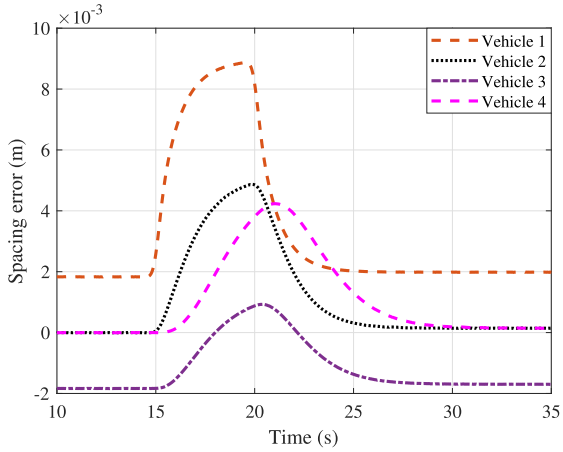

FIGURE 7. Plots showing spacing error attenuation for a heterogeneous platoon.

D. PFSS CONTROLLER PERFORMANCE UNDER HETEROGENEOUS LOADING CONDITIONS

A heterogeneous condition where (follower) vehicle 1 was overloaded by 40% and vehicle 3 underloaded by 40% [43] has also been considered to evaluate for the robustness of the proposed method to vehicle mass variations. The proposed approach was found to be performing well under such conditions, and the error attenuation plot for the heterogeneously loaded platoon is presented in Fig. 7. Similar to the homogeneous case, the errors are bounded to smaller values (order of 10^{-3}) and were found to be attenuating along the length of the platoon.

Table 2 presents the performance evaluation of the proposed PFSS controller for different operating scenarios. Both homogeneous and heterogeneous loading conditions (both overloaded and underloaded) were considered. For each

TABLE 2. Performance evaluation of the proposed PFSS controller for different operating conditions.

Tracking profile		μ	θ	Actuator limits (H/NH)	String stable (H/NH)
Accelerating	1 m/s^2	Dry	+	⇓ / ⇓	Yes / Yes
			o	⇓ / ⇓	Yes / Yes
			-	⇓ / ⇓	Yes / Yes
		Wet	+	⇓ / ⇓	Yes / Yes
			o	⇓ / ⇓	Yes / Yes
			-	⇓ / ⇓	Yes / Yes
	2 m/s^2	Dry	+	⇑ / ⇑	No / No
			o	⇓ / ⇑	Yes / No
			-	⇓ / ⇓	Yes / Yes
		Wet	+	⇑ / ⇑	No / No
			o	⇑ / ⇑	No / No
			-	⇓ / ⇑	Yes / No
Decelerating	-1 m/s^2	Dry	+	⇓ / ⇓	Yes / Yes
			o	⇓ / ⇓	Yes / Yes
			-	⇓ / ⇓	Yes / Yes
		Wet	+	⇓ / ⇓	Yes / Yes
			o	⇓ / ⇓	Yes / Yes
			-	⇓ / ⇓	Yes / Yes
	-2 m/s^2	Dry	+	⇓ / ⇓	Yes / Yes
			o	⇓ / ⇓	Yes / Yes
			-	⇓ / ⇑	Yes / No
		Wet	+	⇓ / ⇑	Yes / No
			o	⇑ / ⇑	No / No
			-	⇑ / ⇑	No / No

μ - Road friction coefficient with Dry: $\mu = 0.8$, and Wet: $\mu = 0.4$;
θ - Road gradient with (+, o, -) indicating (+5°, 0°, -5°) road slope values;
H/NH - Homogeneous/Heterogeneous loading condition;
⇓: Within actuator limit, ⇑: Outside actuator limit.

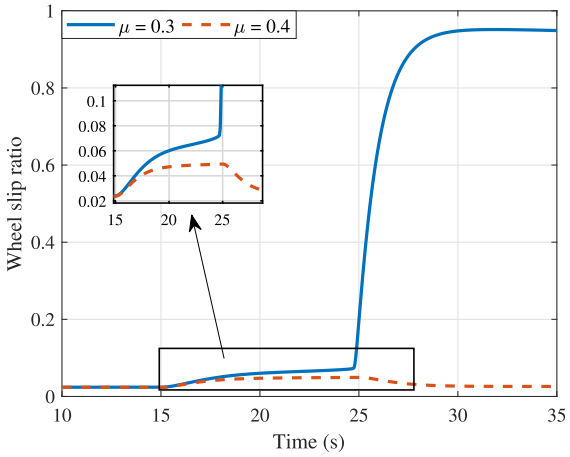

FIGURE 8. Wheel slip ratio for different road surfaces.

set, along with string stability, the magnitude of the torque inputs was also checked for possible actuator limit infringements. For profiles with 1 m/s^2 and -1 m/s^2 acceleration, the proposed PFSS controller could ensure string stable operation (with torque inputs well within the physical limits of actuator) for both homogeneous and heterogeneous loading conditions. The impact of various operating conditions is visible from Table 2. For instance, consider the case where the platoon leader is accelerating from 10 m/s to 15 m/s at 2 m/s^2 on a straight and level dry road. While the proposed PFSS controller could ensure string stable operation for a homogeneously loaded platoon, the same was not ensured for a heterogeneous platoon. For overloaded vehicles, the torque input exceeded the actuator physical limit in this case and resulted in string instability.

Remark 1: It can be observed that for $\mu < 0.4$, the proposed approach could not ensure string stability in all the considered scenarios. A scenario where vehicle 1 in the platoon lost its stability due to an increase in wheel slip ratio is shown in Fig. 8. For $\mu < 0.4$, the wheel slip ratio increases (Fig. 8), leading to wheel spin and potential vehicle instability. This caused the vehicles to collide, resulting in string instability. A similar situation exists in panic braking scenarios, which could be addressed by integrating with a suitable Wheel Slip Regulation (WSR) algorithm.

V. CONCLUSION

A string stable controller design methodology for HCRV platoons using artificial potential function has been proposed. This approach was found to be efficient in attenuating the spacing error propagation by controlling the individual vehicle instantaneous spacing error magnitudes. The proposed controller was seen to possess attributes such as lesser data requirement from neighboring vehicles, actuator feasible control input magnitudes, and a simpler control structure. Due to these attributes, this approach could potentially be taken towards the real-time implementation of heavy vehicle platooning for long-haul freight transportation. Integration of the proposed PFSS control algorithm with a suitable Wheel Slip Regulation (WSR) algorithm would be considered as a potential immediate future scope of this study.

REFERENCES

[1] A. Alam, B. Besselink, V. Turri, J. Mårtensson, and K. H. Johansson, "Heavy-duty vehicle platooning for sustainable freight transportation: A cooperative method to enhance safety and efficiency," *IEEE Control Syst. Mag.*, vol. 35, no. 6, pp. 34–56, Dec. 2015.

[2] K. Liang, J. Mårtensson, and K. H. Johansson, "Heavy-duty vehicle platoon formation for fuel efficiency," *IEEE Trans. Intell. Transp. Syst.*, vol. 17, no. 4, pp. 1051–1061, Apr. 2016.

[3] V. Turri, B. Besselink, and K. H. Johansson, "Cooperative look-ahead control for fuel-efficient and safe heavy-duty vehicle platooning," *IEEE Trans. Control Syst. Technol.*, vol. 25, no. 1, pp. 12–28, Jan. 2017.

[4] S. W. Smith, Y. Kim, J. Guanetti, R. Li, R. Firoozi, B. Wootton, A. A. Kurzhanskiy, F. Borrelli, R. Horowitz, and M. Arcak, "Improving urban traffic throughput with vehicle platooning: Theory and experiments," *IEEE Access*, vol. 8, pp. 141208–141223, 2020.

[5] D. Swaroop and J. K. Hedrick, "String stability of interconnected systems," *IEEE Trans. Autom. Control*, vol. 41, no. 3, pp. 349–357, Mar. 1996.

[6] A. Tuchner and J. Haddad, "Vehicle platoon formation using interpolating control: A laboratory experimental analysis," *Transp. Res. C, Emerg. Technol.*, vol. 84, pp. 21–47, Nov. 2017.

[7] J. Ploeg, D. P. Shukla, N. van de Wouw, and H. Nijmeijer, "Controller synthesis for string stability of vehicle platoons," *IEEE Trans. Intell. Transp. Syst.*, vol. 15, no. 2, pp. 854–865, Apr. 2014.

[8] X. Guo, J. Wang, F. Liao, and R. S. H. Teo, "Distributed adaptive integrated-sliding-mode controller synthesis for string stability of vehicle platoons," *IEEE Trans. Intell. Transp. Syst.*, vol. 17, no. 9, pp. 2419–2429, Sep. 2016.

[9] R. Merco, F. Ferrante, and P. Pisu, "A hybrid controller for DOS-resilient string-stable vehicle platoons," *IEEE Trans. Intell. Transp. Syst.*, vol. 22, no. 3, pp. 1697–1707, Mar. 2021.

[10] E. Semsar-Kazerooni, J. Verhaegh, J. Ploeg, and M. Alirezaei, "Cooperative adaptive cruise control: An artificial potential field approach," in *Proc. IEEE Intell. Vehicles Symp. (IV)*, Jun. 2016, pp. 361–367.

[11] E. Semsar-Kazerooni, K. Elferink, J. Ploeg, and H. Nijmeijer, "Multi-objective platoon maneuvering using artificial potential fields," *IFAC-PapersOnLine*, vol. 50, no. 1, pp. 15006–15011, Jul. 2017.
[12] R. Kianfar, P. Falcone, and J. Fredriksson, "A control matching model predictive control approach to string stable vehicle platooning," *Control Eng. Pract.*, vol. 45, pp. 163–173, Dec. 2015.
[13] G. J. L. Naus, R. P. A. Vugts, J. Ploeg, M. J. G. van de Molengraft, and M. Steinbuch, "String-stable CACC design and experimental validation: A frequency-domain approach," *IEEE Trans. Veh. Technol.*, vol. 59, no. 9, pp. 4268–4279, Nov. 2010.
[14] E. van Nunen, J. Reinders, E. Semsar-Kazerooni, and N. van de Wouw, "String stable model predictive cooperative adaptive cruise control for heterogeneous platoons," *IEEE Trans. Intell. Vehicles*, vol. 4, no. 2, pp. 186–196, Jun. 2019.
[15] B. Peng, D. Yu, H. Zhou, X. Xiao, and Y. Fang, "A platoon control strategy for autonomous vehicles based on sliding-mode control theory," *IEEE Access*, vol. 8, pp. 81776–81788, 2020.
[16] L. Xiao and F. Gao, "Practical string stability of platoon of adaptive cruise control vehicles," *IEEE Trans. Intell. Transp. Syst.*, vol. 12, no. 4, pp. 1184–1194, Dec. 2011.
[17] W. B. Dunbar and D. S. Caveney, "Distributed receding horizon control of vehicle platoons: Stability and string stability," *IEEE Trans. Autom. Control*, vol. 57, no. 3, pp. 620–633, Mar. 2012.
[18] B. Németh and P. Gáspár, "Optimised speed profile design of a vehicle platoon considering road inclinations," *IET Intell. Transp. Syst.*, vol. 8, no. 3, pp. 200–208, May 2014.
[19] D. Chen, S. Ahn, M. Chitturi, and D. Noyce, "Truck platooning on uphill grades under cooperative adaptive cruise control (CACC)," *Transp. Res. C, Emerg. Technol.*, vol. 94, pp. 50–66, Sep. 2018.
[20] J.-W. Kwon and D. Chwa, "Adaptive bidirectional platoon control using a coupled sliding mode control method," *IEEE Trans. Intell. Transp. Syst.*, vol. 15, no. 5, pp. 2040–2048, Oct. 2014.
[21] V. S. Dolk, J. Ploeg, and W. P. M. H. Heemels, "Event-triggered control for string-stable vehicle platooning," *IEEE Trans. Intell. Transp. Syst.*, vol. 18, no. 12, pp. 3486–3500, Dec. 2017.
[22] C. Zhai, F. Luo, and Y. Liu, "Cooperative look-ahead control of vehicle platoon travelling on a road with varying slopes," *IET Intell. Transp. Syst.*, vol. 13, no. 2, pp. 376–384, Feb. 2019.
[23] G. Guo and D. Li, "Adaptive sliding mode control of vehicular platoons with prescribed tracking performance," *IEEE Trans. Veh. Technol.*, vol. 68, no. 8, pp. 7511–7520, Aug. 2019.
[24] L. Xu, W. Zhuang, G. Yin, and C. Bian, "Stable longitudinal control of heterogeneous vehicular platoon with disturbances and information delays," *IEEE Access*, vol. 6, pp. 69794–69806, 2018.
[25] F. Gao, S. E. Li, Y. Zheng, and D. Kum, "Robust control of heterogeneous vehicular platoon with uncertain dynamics and communication delay," *IET Intell. Transp. Syst.*, vol. 10, no. 7, pp. 503–513, Sep. 2016.
[26] Z. Yang, J. Huang, D. Yang, and Z. Zhong, "Collision-free ecological cooperative robust control for uncertain vehicular platoons with communication delay," *IEEE Trans. Veh. Technol.*, vol. 70, no. 3, pp. 2153–2166, Mar. 2021.
[27] C. Zhai, X. Chen, C. Yan, Y. Liu, and H. Li, "Ecological cooperative adaptive cruise control for a heterogeneous platoon of heavy-duty vehicles with time delays," *IEEE Access*, vol. 8, pp. 146208–146219, 2020.
[28] K. B. Devika, G. Rohith, V. R. S. Yellapantula, and S. C. Subramanian, "A dynamics-based adaptive string stable controller for connected heavy road vehicle platoon safety," *IEEE Access*, vol. 8, pp. 209886–209903, 2020.
[29] O. Khatib, "Real-time obstacle avoidance for manipulators and mobile robots," in *Autonomous Robot Vehicles*. New York, NY, USA: Springer, 1986, pp. 396–404.
[30] E. Rimon and D. E. Koditschek, "Exact robot navigation using artificial potential functions," *IEEE Trans. Robot. Automat.*, vol. 8, pp. 501–518, 1992.
[31] Y. Wang and X. Sun, "Formation control of multi-UAV with collision avoidance using artificial potential field," in *Proc. 11th Int. Conf. Intell. Hum.-Mach. Syst. Cybern. (IHMSC)*, vol. 1, Aug. 2019, pp. 296–300.
[32] G. Rohith and M. Vadali, "A quasi-centralized collision-free path planning approach for multi-robot systems," 2021, *arXiv:2103.10316*.
[33] P. Vadakkepat, K. C. Tan, and W. Ming-Liang, "Evolutionary artificial potential fields and their application in real time robot path planning," in *Proc. Congr. Evol. Comput.*, vol. 1, Jul. 2000, pp. 256–263.
[34] H. Adeli, M. Tabrizi, A. Mazloomian, E. Hajipour, and M. Jahed, "Path planning for mobile robots using iterative artificial potential field method," *Int. J. Comput. Sci. Issues*, vol. 8, no. 4, p. 28, Jul. 2011.
[35] T. Weerakoon, K. Ishii, and A. A. F. Nassiraei, "An artificial potential field based mobile robot navigation method to prevent from deadlock," *J. Artif. Intell. Soft Comput. Res.*, vol. 5, no. 3, pp. 189–203, Sep. 2015.
[36] S. Feng, Y. Qian, and Y. Wang, "Collision avoidance method of autonomous vehicle based on improved artificial potential field algorithm," *Proc. Inst. Mech. Eng., D, J. Automobile Eng.*, vol. 235, no. 14, pp. 3416–3430, Dec. 2021.
[37] R. Rajamani, *Vehicle Dynamics and Control*. Cham, Switzerland: Springer, 2011.
[38] H. Pacejka, *Tire and Vehicle Dynamics*. Amsterdam, The Netherlands: Elsevier, 2005.
[39] N. Sridhar, K. V. Subramaniyam, S. C. Subramanian, G. Vivekanandan, and S. Sivaram, "Model based control of heavy road vehicle brakes for active safety applications," in *Proc. 14th IEEE India Council Int. Conf. (INDICON)*, Dec. 2017, pp. 1–6.
[40] L. C. Davis, "Stability of adaptive cruise control systems taking account of vehicle response time and delay," *Phys. Lett. A*, vol. 376, nos. 40–41, pp. 2658–2662, Aug. 2012.
[41] M. W. Hancock and B. Wright, *A Policy on Geometric Design of Highways and Streets*. Washington, DC, USA: American Association of State Highway and Transportation, 2013.
[42] L. Xu, L. Y. Wang, G. Yin, and H. Zhang, "Communication information structures and contents for enhanced safety of highway vehicle platoons," *IEEE Trans. Veh. Technol.*, vol. 63, no. 9, pp. 4206–4220, Nov. 2014.
[43] D. Savio, K. Kavinmathi, J. M. Krishnan, and S. C. Subramanian, "Influence of truck acceleration on dynamic load transfer to pavement," in *Airfield and Highway Pavements 2019: Design, Construction, Condition Evaluation, and Management of Pavements*. Reston, VA,USA: American Society of Civil Engineers, 2019, pp. 72–80.

K. B. DEVIKA (Member, IEEE) received the Ph.D. degree in control systems from the National Institute of Technology, Calicut. She is currently a Postdoctoral Fellow with the Department of Engineering Design, Indian Institute of Technology Madras, India. Her research interests include control of automotive and transportation systems and sliding mode control.

G. ROHITH (Member, IEEE) received the Ph.D. degree in aerospace engineering from the Indian Institute of Technology Madras. He is currently a Postdoctoral Fellow with the College of Engineering, Mathematics and Physical Sciences, University of Exeter, U.K. His research interests include dynamics and control of automotive and aerospace systems and clean mobility.

SHANKAR C. SUBRAMANIAN (Senior Member, IEEE) received the Ph.D. degree from Texas A&M University, USA. He is currently a Professor and a V. Ramamurti Faculty Fellow with the Department of Engineering Design, Indian Institute of Technology Madras, Chennai, India. His research interests include dynamics and control with applications to automotive and transportation systems.